



OPEN Hypoglycemia and hyperinsulinemia induced by phenolic uremic toxins in CKD and DKD patients

Yoshiyasu Tongu^{1,2}, Tomoko Kasahara^{2,3}, Yasutoshi Akiyama⁴, Takehiro Suzuki^{2,3,5}, Hsin-Jung Ho^{2,3,10}, Yotaro Matsumoto⁴, Ryota Kujirai⁴, Koichi Kikuchi^{2,3}, Koji Nata⁶, Makoto Kanzaki⁷, Kenshin Suzuki^{1,2}, Shun Watanabe^{2,3}, Chiharu Kawabe², Yui Miyata^{2,8}, Shun Itai², Takafumi Toyohara^{2,3}, Chitose Suzuki², Tetsuhiro Tanaka³, Jun Wada⁹, Yoshihisa Tomioka⁴ & Takaaki Abe^{2,3,5}✉

Patients with end-stage renal disease have lower fasting plasma glucose and HbA1c levels, with significantly higher insulin levels. For a long time, it has been believed that this higher insulin level in renal failure is due to decreased insulin clearance caused by reduced renal function. However, here we reported that accumulation of the gut microbiota-derived uremic toxin, phenyl sulfate (PS) in the renal failure, increased insulin secretion from the pancreas by enhanced glucose-stimulated insulin secretion. Other endogenous sulfides compounds which accumulated as in the renal failure also increased glucose-stimulated insulin secretion from β -cell. With RNA-seq analyses and gene knock down, we demonstrated that insulin secretion evoked by PS was mediated by Ddah2. In addition, we also found that PS increased insulin resistance through lncRNA expression and Erk phosphorylation in the adipocytes. To confirm the relationship between PS and glucose metabolism in human, we recruited 2 clinical cohort studies (DKD and CKD) including 462 patients, and found that there was a weak negative correlation between PS and HbA1c. Because these trials did not measure fasting insulin level, we alternatively used the urinary C-peptide/creatinine ratio (UCPCR) as an indicator of insulin resistance. We found that PS may induce insulin resistance in patients with eGFR < 60 mL/min/1.73 m². These data suggest that the accumulation of uremic toxins modulates glucose metabolism and induced insulin resistance in CKD and DKD patients. Considering HbA1c as a reflection of chronic hyperglycemia and UCPCR as a reflection of chronic hyperinsulinemia, our findings indicate that PS is negatively associated with hyperglycemia independent of CKD, and positively associated with hyperinsulinemia in DKD patients.

Keywords CKD, DKD, Phenyl sulfate, Uremic toxin, Insulin secretion, Insulin resistance, Gut microbiota

Abbreviations

BUN	blood urea nitrogen
CE-TOFMS	capillary electrophoresis with electrospray ionization time-of-flight mass spectrometry
CKD	chronic kidney disease
Cre	creatinine
Ddah2	dimethylarginine dimethylaminohydrolase 2

¹Tohoku University School of Medicine, Sendai, Japan. ²Department of Clinical Biology and Hormonal Regulation, Tohoku University Graduate School of Medicine, Sendai, Japan. ³Division of Nephrology, Endocrinology, and Vascular Medicine, Tohoku University Graduate School of Medicine, Sendai, Japan. ⁴Laboratory of Oncology, Pharmacy Practice and Sciences, Tohoku University Graduate School of Pharmaceutical Sciences, Sendai, Japan. ⁵Division of Medical Science, Tohoku University Graduate School of Biomedical Engineering, Sendai, Japan. ⁶Department of Medical Biochemistry, School of Pharmacy, Iwate Medical University, Morioka, Japan. ⁷Department of Biomedical Engineering, Tohoku University, Sendai, Japan. ⁸Department of Surgery, Tohoku University Graduate School of Medicine, Sendai, Japan. ⁹Department of Nephrology, Rheumatology, Endocrinology and Metabolism, Okayama University Graduate School of Medicine, Dentistry and Pharmaceutical Sciences, Okayama, Japan. ¹⁰Present address: Faculty of Health Sciences, Hokkaido University, Sapporo, Japan. ✉email: takaaki.abed1@tohoku.ac.jp

DKD	diabetic kidney disease
ESRD	end-stage renal disease
GSIS	glucose-stimulated insulin secretion
GTT	glucose tolerance test
HF	high-fat
ipITT	intraperitoneal insulin tolerance test
lncRNA	long non-coding RNA
Prkag1	protein kinase AMP-activated non-catalytic subunit gamma 1
PS	phenyl sulfate
RF	renal failure
U-CARE	Urinary Biomarker for Continuous and Rapid Progression of Diabetic Nephropathy
UCPCR	urinary C-peptide/creatinine ratio
WAT	white adipose tissue

The kidney plays a crucial role in insulin metabolism, including the filtration of insulin by the glomerulus and its degradation in the tubules. Declining kidney function significantly alters this process¹. Chronic kidney disease (CKD) is well-known to be associated with hypoglycemia, particularly in end-stage renal disease (ESRD), as supported by clinical data showing lower fasting plasma glucose (FPG) and HbA1c levels, along with markedly higher insulin levels in these patients^{2–4}. Initially, this elevated insulin level was thought to result from reduced insulin clearance due to impaired kidney filtration capacity⁵.

However, recent studies have provided conflicting evidence, showing increased C-peptide levels in ESRD patients³. This finding has led to considerations of additional factors, such as nutritional deterioration, effects of diabetes medications⁶, and reduced gluconeogenesis associated with renal failure⁷. Beyond hypoglycemia, the decline in kidney function is also implicated in inducing insulin resistance, further complicating glucose metabolism⁸.

Diabetic kidney disease (DKD), characterized by renal dysfunction and difficulty in glycemic control⁹, often involves the destruction of podocytes, a key element in its pathophysiology¹⁰. Our previous research has identified phenyl sulfate (PS), a gut microbiota-derived uremic toxin that accumulates with declining kidney function, as a critical factor in DKD. PS not only serves as a marker for the diagnosis and prognosis of DKD but also exerts harmful effects on podocytes¹¹. Additionally, PS accumulation in CKD has been found to damage podocytes and worsen DKD. Notably, we observed a negative correlation between PS levels and HbA1c, suggesting a potential role of PS in glucose metabolism¹¹.

Based on these insights, the current study investigates the effects of PS on insulin secretion and insulin resistance. We explore how PS enhances insulin secretion from the islets of Langerhans and examine its relationship with renal dysfunction in DKD. These findings provide a foundation for developing new therapeutic strategies to improve glycemic control in patients with DKD.

Results

PS induced insulin secretion but not resistance in normal mice

In both diabetic mice and human DKD subjects, we previously reported that PS exhibits nephrotoxic effects by mesangial damage with increased albuminuria¹¹. To clarify the relationship between PS and insulin metabolism, we firstly examined the effect of PS on healthy mice. PS was orally administered for 5 weeks (50 mg/kg/day), and it was found that there was no significant change in body weight, albuminuria, or the mesangial region in the kidney (Fig. 1A, B, C). In the PS-treated group, fasting glucose was decreased (Fig. 1D) and also the fasting insulin level was increased (Fig. 1E). Under the condition, we performed a glucose tolerance test (GTT). The glucose level and glucose induced insulin secretion were not changed between control- and PS-treated group (Fig. 1F). We also performed intraperitoneal insulin tolerance test (ipITT; 2 U/kg insulin), to examine the insulin sensitivity. The ipITT showed no significant difference in the ratio of change in blood glucose between the groups (Fig. 1G). These data demonstrated that PS stimulates insulin secretion without altering insulin sensitivity in normal mice. To uncover the underlying mechanism, we measured the size of the pancreatic islets, which is considered an indicator of insulin secretion in humans¹². In PS-treated mice, the size of insulin-positive β -cell significantly increased (Fig. 1H). In contrast, no histological changes were observed in adipocytes, liver, or skeletal muscle, which are typically implicated in insulin resistance (Fig. 1I). These data suggested that PS exerts a hypoglycemic effect by promoting insulin secretion.

PS induced insulin secretion and resistance in the diabetic mouse

To further examine the effect of PS on insulin metabolism, we administered PS to KKAY mice, a type 2 DM model, fed a high-fat (HF) diet (PS-treated KKAY-HF mice)¹³. After 5 weeks of administration (50 mg/kg/day), albuminuria significantly increased, unlike that in normal mice although there was no change in the body weight (Fig. 2A, B). Enlargement of the mesangial region was also observed (Fig. 2C). Concerning glucose metabolism, in the PS-treated group, fasting glucose level was also decreased (Fig. 2D) and basal insulin level was tended to be higher in the PS group ($p = 0.05$, Fig. 2E). Under the condition, we further performed the GTT (2 g/kg) (Fig. 2F). As a result, glucose levels did not differ between the groups; however, insulin level was slightly higher in the PS-treated group but not significant (Fig. 2F). Next, we examined ipITT to determine whole-body sensitivity (Fig. 2G). The results showed that the glucose level after insulin injection (2 U/kg) was significantly increased in the ratio of change in blood glucose in PS-treated KKAY-HF mice compared with that in control mice, further suggesting insulin resistance (Fig. 2G). Histologically, the number of insulin-positive β -cells was increased in the pancreas of PS-treated KKAY-HF mice, suggesting that the insulin-secretion capacity of the PS-treated group was higher (Fig. 2H). Because liver and muscle are involved in the insulin resistance, we next

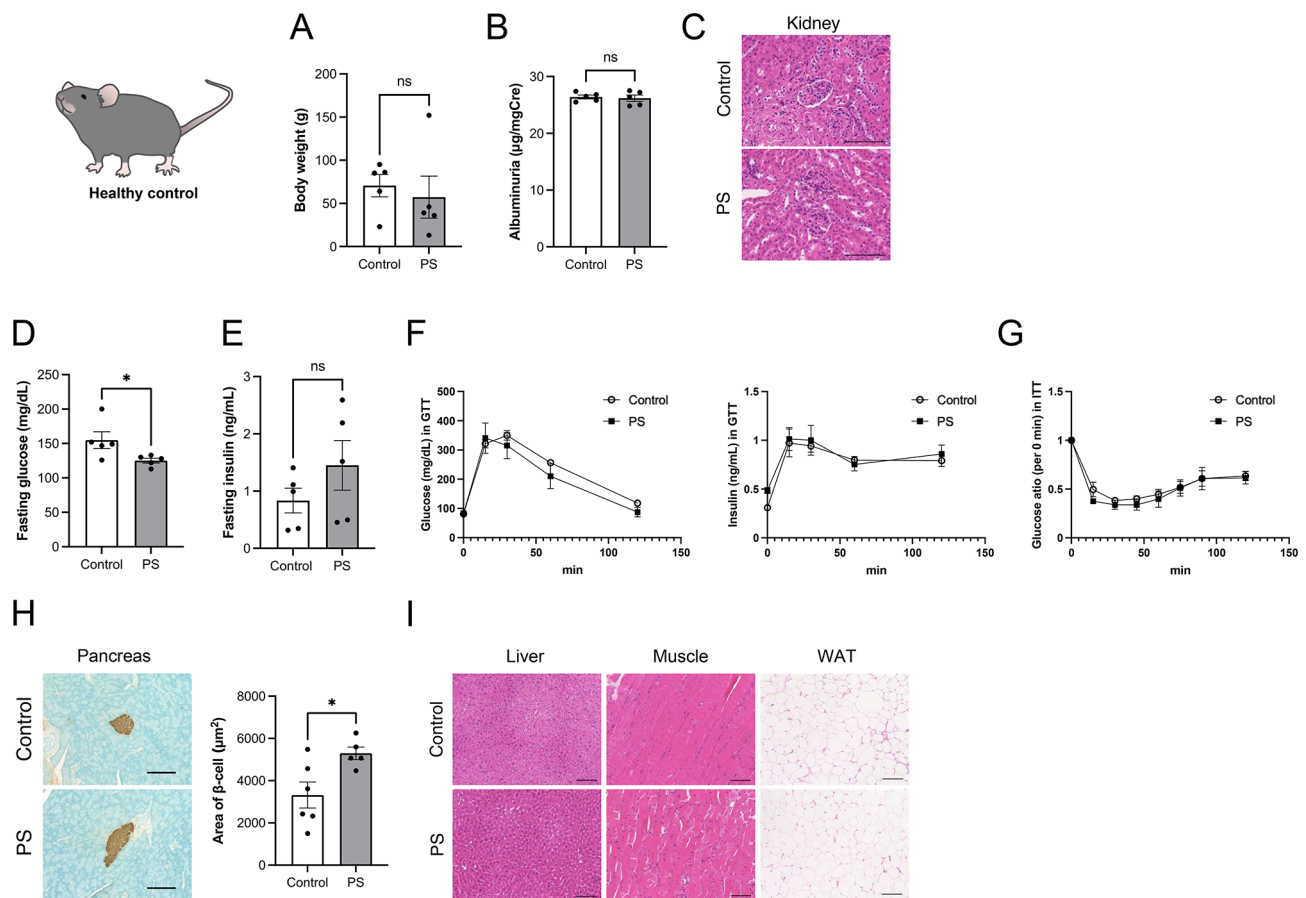


Fig. 1. PS administration with healthy C57BL/6J mice. (A) Body weight and (B) albuminuria change with PS administration in healthy C57BL/6J mice. ($n = 3$ in each groups). (C) Histological analysis of kidney of the mice. (D) Fasting glucose and (E) insulin level after 5-week PS administration. (F) Glucose change and insulin change in GTT test. (G) Glucose level change in ipITT test. (H) Histological image and analysis of pancreas and (I) the image of liver, muscle and white adipose tissue (WAT) of the normal mice. * $p < 0.05$, ** $p < 0.01$, *** $p < 0.001$ vs. Control, student t -test. Scale bars; 100 μm , 10x objective lens was used.

examine the histological difference in the liver and muscle and no significant change was observed (Fig. 2I). It is also well-known that hypertrophy of adipocytes is the main mechanism of adult fat mass expansion and insulin resistance^{14,15}, so, we further measured the size of the white adipose tissue (WAT). In KKAY-HF mice treated with PS, the size of adipocytes increased and the number of adipocyte per WAT area decreased (Fig. 2I). Collectively, these data suggest that PS has two effects: (i) it increases insulin secretion from islets, and (ii) it induces insulin resistance in adipocytes.

PS stimulated insulin secretion in the pancreatic β -cells

To elucidate the relationship between PS and insulin secretion, we evaluated the effects of PS on glucose-induced insulin secretion (GSIS) in a rat β -cell line (INS-1e)^{16,17}. In INS-1e cells, 20 mM glucose showed a 4.5-fold increase in insulin secretion compared to 2 mM glucose. We decided the physiological concentration of PS in humans, based on our previous report¹¹. The concentration of PS in the ESRD patients exhibited approximately 100 μM ¹⁸ and we also adapted 1 mM PS as maximum physiological concentration.

Under these conditions, PS (10 μM) significantly enhanced 20 mM GSIS by 1.3-fold, and 100 μM PS further increased GSIS by 2.1-fold (Fig. 3A). To confirm the stimulatory effect of PS on insulin secretion, we examined GSIS in mouse isolated pancreatic islets¹⁹. Isolated mouse islets in a medium with a glucose level of 2.8 mM were incubated with 11 mM glucose, with or without PS (100 μM), and the secreted insulin was measured. As shown in Fig. 3B, PS (100 μM) stimulated GSIS by 2.8-fold compared to islets without PS. In contrast, the pancreatic insulin content was not changed by PS stimulation (Fig. 3C). These data suggest that PS stimulates just insulin secretion by stimulating secretion from islets, and not by increasing insulin production.

Endogenous PS analogs stimulated insulin secretion from the islet

PS is a sulfurized metabolite of phenol generated by dietary tyrosine in the gut microbiota¹¹. Various sulfurized endogenous and exogenous compounds exist in the human body, and we found that uremic toxins, including phenol and sulfurized derivatives, accumulate in the circulation of patients with CKD and DKD patients²⁰.

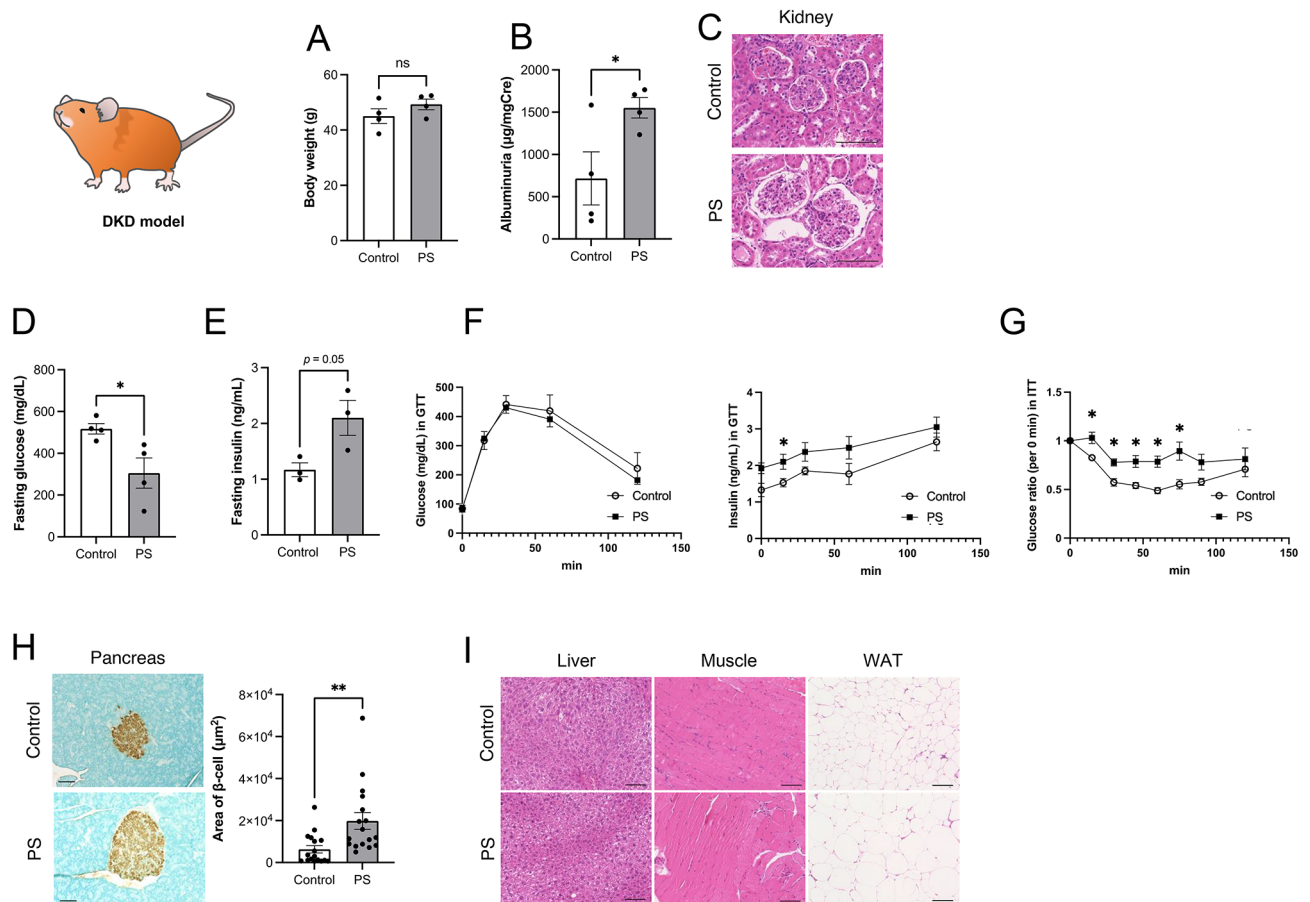


Fig. 2. PS administration with KKAY-HF diet mice. (A) Body weight and (B) albuminuria of PS administration with normal KKAY-HF diet mice. (*n* = 3 in each group). (C) Histological analysis of kidney of the mice. (D) Fasting glucose and (E) insulin level after 5-week PS administration. (F) Glucose change and insulin change in GTT test. (G) Glucose level change in ITT test. (H) Histological image and analysis of pancreas and (I) liver, muscle and white adipose tissue (WAT) of the KKAY-HF mice. **p* < 0.05, ***p* < 0.01 vs Control, student *t*-test. Scale bars; 100 μm, 10× objective lens was used.

In addition, sulfation is an important metabolic pathway for xenobiotics, hormones, and neurotransmitters in humans and is catalyzed by cytosolic sulfotransferase²¹. By searching the Human Metabolome Database (HMDB, <https://hmdb.ca>), we identified 11 endogenous sulfate compounds (*p*-cresyl sulfate, *p*-nitrophenyl sulfate, *o*-cresyl sulfate, androsterone sulfate, dihydroxy ferulic acid 4-sulfate, testosterone sulfate, *o*-methoxyphenyl sulfate, vanillin sulfate, 4-methoxyphenylethanyl sulfate, pyrocatechol sulfate, and 4-acetaminophen sulfate) in humans. We also found four sulfate analogs (2-naphthyl sulfate, 8-quinoliny sulfate, 1-naphthyl sulfate, and cyclohexany sulfate) synthesized in humans, and total 15 sulfate compounds (Table 1) were analyzed for their effect on GSIS. Among the 11 endogenous compounds, eight compounds (*p*-cresyl sulfate, *p*-nitrophenyl sulfate, *o*-cresyl sulfate, androsterone sulfate, dihydroxyferulic acid 4-sulfate, testosterone sulfate, *o*-methoxyphenyl sulfate, and 4-methoxyphenylethanyl sulfate) and PS enhanced 20 mM glucose-stimulated GSIS (100 μM, Fig. 3D). In addition, 2-naphthyl sulfate, 8-quinoliny sulfate, 1-naphthyl sulfate, and cyclohexany sulfate also increased the concentration of 20 mM GSIS. Because some PS, *p*-cresyl sulfate, androsterone sulfate, and *o*-methoxyphenyl sulfate were found as uremic toxins and the concentration was increased in CKD and DKD^{20,22}, the accumulation of these compounds in CKD and DKD patients may enhance the secretion of insulin or inducing insulin resistance in CKD and DKD.

Stimulated insulin secretion through the Ddah2 and AMPK pathways in the pancreas

To clarify the mechanism underlying the effect of PS on insulin secretion, we performed RNA sequencing (RNA-seq) of INS-1e cells treated with or without PS (100 μM). A result of 29,504 genes was detected by RNA-seq, and the enhanced volcano plots showed differences in gene expression in each group (Fig. 3E). Among the genes, we identified two that exhibited significant changes by PS exposure ($|\log_2FC| > 2.5$, $-\log_{10}P > 2.5$, normalized read counts > 0). The heatmap also showed that the top 25 transcripts were upregulated (Fig. 3F) or downregulated (Fig. 3I) following PS treatment (Fig. 3F, I). Among these, dimethylarginine dimethylaminohydrolase 2 (Ddah2) was up-regulated by PS (Fig. 3G). Ddah2 has been reported to be an enzyme that regulates the metabolism of nitric oxide and has been identified as one of the regulators of insulin secretion in the pancreas²³. It enhances

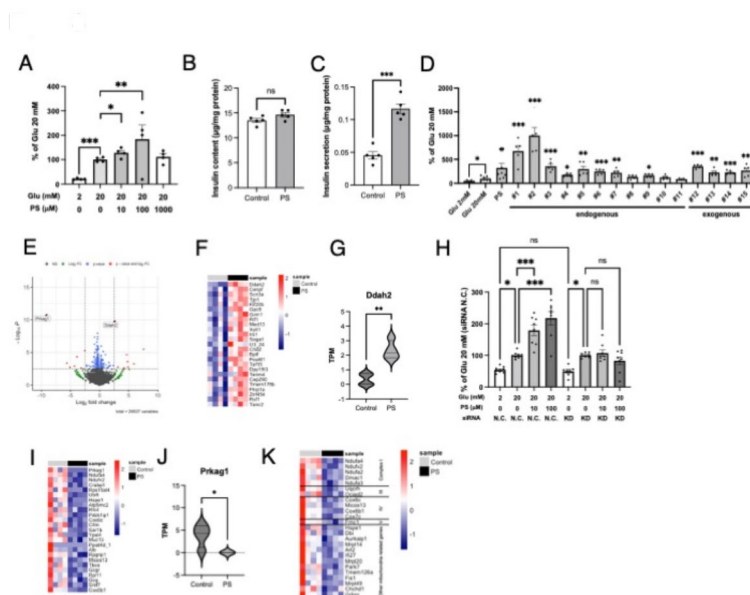


Fig. 3. PS and PS analogs increased insulin secretion in vitro and RNA-seq revealed the mechanism. (A) GSIS in INS-1e and (B) isolated mouse pancreas were performed using various concentrations of PS. (C) Insulin levels after PS administration. (D) GSIS was performed with the PS analogs. RNA-seq was performed on PS-treated ins1e cells. (E) Volcano plot. (F) Heatmap of the top 25 transcripts upregulated by the PS treatment. (G) TPM of Ddah2 changed by PS. (H) GSIS in Ddah2-Knock down (KD) INS-1e cells. (I) Heatmap of the top 25 transcripts downregulated by the PS treatment. (J) Changes in the TPM in Prkag1. (K) Mitochondria-related genes altered by PS are shown in a heatmap. * $p < 0.05$, ** $p < 0.01$, *** $p < 0.001$ vs. Control (Glu 20 mM), student t -test (for A, B, C, D), One-way ANOVA Tukey test (for H) and false discovery rate (FDR) correction method. (for G, J)

insulin secretion by regulating transcription through a Sirt1-dependent mechanism. To determine whether Ddah2 mediates PS-induced insulin secretion, we knocked down the Ddah2 gene using siRNA and performed GSIS assay (Fig. 3H). The knockdown efficiency is shown in Supplemental Fig. 1. As a negative control, we used a scramble siRNA that does not affect Ddah2 expression. As a result, when Ddah2 was knocked down in INS-1e cells, PS-mediated GSIS increase was cancelled both in 10 and 100 μ M glucose. These data suggested that the Ddah2 may affect the PS-induced insulin secretion.

Concerning genes down regulated by PS (Fig. 3I), we also found that Protein Kinase AMP-Activated Non-Catalytic Subunit Gamma 1 (Prkag1) was downregulated by PS treatment (Fig. 3J). Prkag1 is a component of AMPK subunits, and downregulation of Prkag1 and subsequent AMPK downregulation promotes the mTOR pathway²⁴, which is known to increase insulin secretion²⁵. These data further suggested the involvement of Prkag1 in insulin secretion mediated by PS.

Recently, we reported that PS induces mitochondrial damage in podocytes and increases albuminuria in DKD¹¹. So, we focused on mitochondria-related genes and comprehensively analyzed the RNA-seq, shown in the heatmap (Fig. 3K). By PS treatment, mitochondrial respiratory chain complexes I (Ndufa4, Ndufv2, Ndufa2, Dmac1, and Ndufa3), III (Uqcrh and Ociad2), IV (Cox6c, Micos13, Cox6b1, and Cox7c), and V (Fmc1) were decreased. These results were consistent with previous experiments showing that PS also acts on the mitochondrial electron transport system¹¹ and suggested that PS increases insulin secretion from pancreatic cells without insulin production.

PS increased insulin resistance through lncRNA expression and Erk1/2 phosphorylation in the adipocyte

To further clarify the mechanism underlying the effect of PS on insulin resistance observed in KKAY model (Fig. 2), we performed RNA-seq using differentiated 3T3-L1 adipocytes treated with and without PS. 41,710 genes were detected by the RNA-seq, and volcano plots showed the difference of gene expression in each group. ($|\log_2\text{FC}| > 2.5$, $-\log_{10}P > 2.5$, normalized read counts > 0 ; Fig. 4A). A heatmap of the top 25 transcripts upregulated by PS is shown (Fig. 4B). The RNA-seq results showed many variations in lncRNA expression. In particular, changes in long non-coding RNA (lncRNA), such as Neat1 or Malat1 were observed, and Gm206877 and Kcnq10t1 are also known as lncRNAs (Fig. 4C and D). Because lncRNAs have been reported to be key substances for adipogenesis or insulin resistance^{26–28}, these data suggest that insulin resistance caused by PS may be due to the action of PS on the transcriptional regulation of lncRNAs in adipocytes. However, among the downregulated genes (Fig. 4E), several genes (e.g., Ccnb1, Mad2l1, Top2a, and Foxm1; Fig. 4F) were involved in cell cycle and cell division processes. A reduction in the expression of these genes suggests decreased cell division. Cell cycle suppression induces obesity and insulin resistance²⁹. The adipocyte changes observed in mice

#	Name	Structure	Endogenous	GSIS
#1	<i>p</i> -cresyl sulfate		○	○
#2	<i>p</i> -nitrophenyl sulfate		○	○
#3	<i>o</i> -cresyl sulfate		○	○
#4	androsterone sulfate		○	○
#5	dihydroferulic acid 4-sulfate		○	○
#6	testosterone sulfate		○	○
#7	<i>o</i> -methoxyphenyl sulfate		○	○
#8	vanillin sulfate		○	
#9	4-methoxyphenylethanyl sulfate		○	○
#10	pyrocatechoyl sulfate		○	
#11	4-acetaminophen sulfate		○	
#12	2-naphthyl sulfate			○
#13	8-quinoliny sulfate			○
#14	1-naphthyl sulfate			○
#15	cyclohexanyl sulfate			○

Table 1. The list of sulfate compounds and those chemical structures

and changes in gene expression suggest that white adipocytes do not divide or swell to induce insulin resistance via adipocytokines.

Adipocytes are one of the major insulin target tissues responsible for maintaining glucose homeostasis. Insulin stimulates GLUT4 translocation to the cell surface, which promotes glucose uptake by the cells and increases insulin sensitivity³⁰, which is also controlled by GLUT4 translocation to the membrane³¹. Recently, we established that differentiated 3T3-L1 adipocytes are equipped with the basic GLUT4 translocation machinery, which can be activated by insulin stimulation^{32,33}. Using this system, we examined the effects of PS on insulin-mediated GLUT4 translocations. As shown in Supplemental Fig. 2A, PS did not affect insulin-mediated GLUT4 translocations. Akt phosphorylation is known to play an important role in GLUT4 translocation. Overexpression of a constitutively active Akt mutant is sufficient to recruit GLUT4 to the cell surface³⁴. So, we examined the effects of PS on Akt phosphorylation induced by 100 nM insulin in 3T3-L1 adipocytes. However, PS did not affect Akt phosphorylation (Supplemental Fig. 2B). It is well known that sortilin plays an essential role in adipocyte and muscle glucose metabolism by controlling GLUT4 localization^{35,36} and impaired insulin signaling is induced by reduced sortilin expression³⁷. Therefore, we further examined the effects of PS on sortilin expression. The protein expression level of sortilin increased after differentiation (day 8), but the expression level

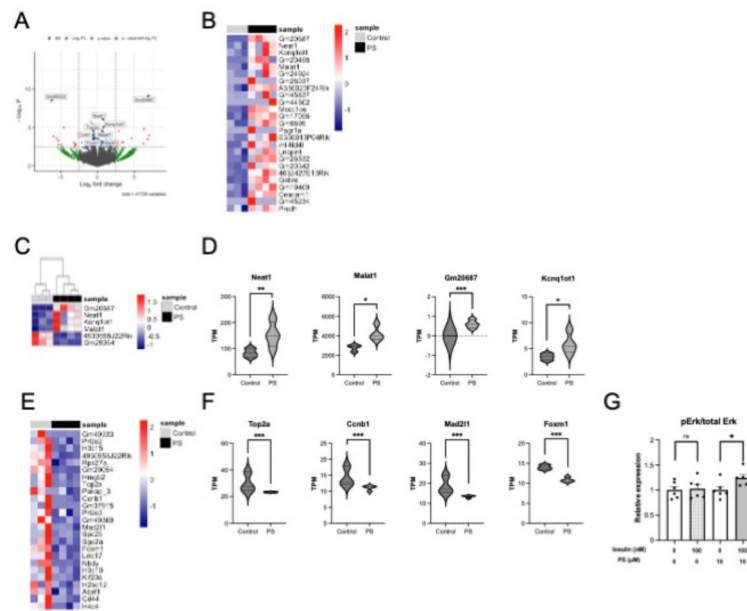


Fig. 4. The mechanism by which PS induced insulin resistance was analyzed with RNA-seq, western blotting, and ELISA. RNA-seq was performed on the PS-treated 3T3-L1 derived adipocyte cells. (A) Volcano plot. (B) Heatmap of the top 25 genes upregulated by PS treatment from RNA-seq data. (C) Heatmap of lncRNAs altered by RNA-seq. (D) TPM changes in the lncRNAs. (E) Heatmap of the top 25 genes downregulated by PS treatment in the RNA-seq data. (F) TPM changes in four genes related to the cell cycle. * $p < 0.05$, ** $p < 0.01$, *** $p < 0.001$ vs. Control, FDR correction method was used. (G) Erk phosphorylation was measured using ELISA. * $p < 0.05$, vs. PS (+) insulin 0 nM, Student's *t*-test.

of sortilin did not change after PS treatment (1–100 μ M, Supplemental Fig. 2C). These data suggest that insulin resistance evoked by PS is not related to GLUT4. The Erk signaling pathway is also a potential cause of insulin resistance in type 2 diabetes^{13,38}. So, we next examined the effects of PS on insulin-induced Erk phosphorylation in differentiated 3T3-L1 adipocytes. Erk phosphorylation induced by insulin was significantly increased by PS (10 μ M) (Fig. 4G). These results suggest that, in addition to the activation of lncRNAs, Erk phosphorylation may also be involved in PS-induced insulin resistance.

Clinical cohort studies show PS changes glucose metabolism by modulating insulin

To confirm the relationship between PS and glucose metabolism from a clinical point of view, we recruited 362 diabetic patients from a DKD patient cohort study, U-CARE (Urinary Biomarker for the Continuous and Rapid Progression of Diabetic Nephropathy) study^{11,39,40}. In this study, patients with DKD had a mean age of 63.3 years and 56.9% were male. The mean blood sugar (BS) concentration was 154.2 ± 56.4 mg/dL and the HbA1c was $7.2 \pm 1.1\%$. eGFR was 73.8 (17.1 – 115.4) mL/min/1.73 m² and the albumin-to-creatinine ratio (ACR) was 11.0 (1.0 – 6407.4) mg/gCr¹⁰. HbA1c is a useful parameter for monitoring serum glycemic control and progression of diabetes mellitus over several months⁴¹. We examined the relationship between PS and HbA1c level in this cohort. As shown in Fig. 5A, there was a weak relationship between HbA1c levels and PS ($p = 0.0169$, $r = -0.1254$). We also classified patients with DKD (eGFR < 60 mL/min/1.73 m²) and found no relationship between PS and HbA1c level (Fig. 5B, $p = 0.8696$, $r = 0.02203$). We further examined the relationship between PS and HbA1c using another cohort of 100 outpatients of Tohoku University Hospital recruited from the non-diabetic population or those with well-controlled diabetes (HbA1c is $5.9 \pm 0.5\%$, average \pm SE, as shown in Table 2). The results showed a weak negative correlation between PS and HbA1c levels in this cohort ($p = 0.022$, $r = -0.2235$; Fig. 5C). A correlation was not obtained when the two previous cohorts were limited to patients with renal failure (eGFR < 60 mL/min/1.73 m², $p = 0.1109$, $r = -0.2466$, Fig. 5D).

Clinically, to examine insulin resistance and PS, HOMA2-IR is used for a standard method⁴². To calculate HOMA2-IR, the value of fasting insulin and glucose values were necessary. However, in the U-CARE (DM) and Tohoku University (non-DM) cohort, we measured BS when patients visited the hospital. To overcome this limitation, the urinary C-peptide/creatinine ratio (UCPCR) is used. It has been reported that UCPCR correlates with HOMA2-IR, fasting C-peptide, and postprandial C-peptide⁴³. Additionally, UCPCR is positively correlated with the prognosis of DKD and coronary heart disease⁴³. Among the 362 patients with DKD who underwent U-CARE, no relationship was observed between plasma PS and UCPCR ($p = 0.456$, $r = -0.04008$; Fig. 5E). Because PS is a uremic toxin and its concentration may increase from CKD grade 3⁴⁴, we classified patients with DKD as having CKD (eGFR < 60 mL/min/1.73 m²). Accordingly, a close relationship was observed between serum PS levels and UCPCR in patients with DKD ($p = 0.023$, $r = 0.3034$) (Fig. 5F). To further confirm the relationship

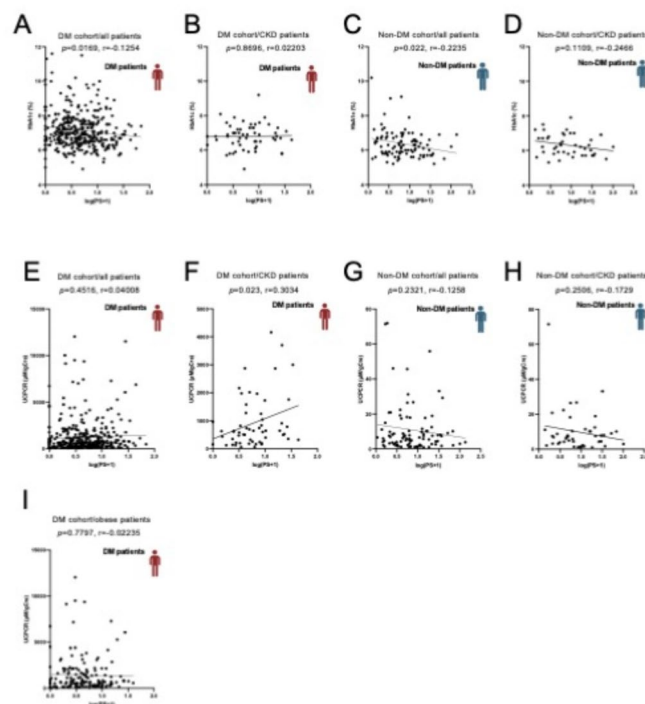


Fig. 5. Relationship between PS and HbA1c or insulin resistance in two clinical cohorts. **(A–D)** Relationship between PS and HbA1c levels. **(A)** All patients in the DM cohort; **(B)** patients with CKD ($\text{eGFR} < 60 \text{ mL/min/1.73 m}^2$) in the DM cohort; **(C)** all patients in the non-DM cohort; and **(D)** patients with CKD ($\text{eGFR} < 60 \text{ mL/min/1.73 m}^2$) in the non-DM cohort. **(E–H)** Relationship between PS and UCPCR. **(E)** All patients in the DM cohort; **(F)** patients with CKD ($\text{eGFR} < 60 \text{ mL/min/1.73 m}^2$) in the DM cohort; **(G)** all patients in the non-DM cohort; and **(H)** patients with CKD ($\text{eGFR} < 60 \text{ mL/min/1.73 m}^2$) in the non-DM cohort. **(I)** Obese patients ($\text{BMI} > 25$) in DM cohort.

		Average \pm SE
PS	(μM)	13.8 ± 17.7
Age	(years)	68.7 ± 12.7
Gender	(M/F)	59 / 41
BMI	(kg/m^2)	24.4 ± 4.1
SBP	(mmHg)	127.6 ± 9.9
DBP	(mmHg)	73.0 ± 6.4
HbA1c	(%)	5.9 ± 23.6
eGFR	(mL/min/1.73m^2)	58.9 ± 23.6
Cr	(g)	1.1 ± 0.7
HDL	(mg/dL)	55.4 ± 15.4
UA	(mg/dL)	6.0 ± 1.6

Table 2. Patients' profile of Tohoku University Hospital cohort

between PS and UCPCR in patients without DM, we used a non-DM cohort from Tohoku University Hospital. There was a slight correlation between PS and UCPCR in all non-diabetic patients ($p = 0.23321$, $r = -0.12$, Fig. 5G), but not in patients with CKD ($\text{eGFR} < 60 \text{ mL/min/1.73 m}^2$) ($p = 0.2506$, $r = -0.1729$, Fig. 5H). These data suggest that PS-induced insulin resistance in DKD patients with $\text{eGFR} < 60 \text{ mL/min/1.73 m}^2$. To further investigate whether obesity could be a factor in determining insulin resistance by PS, the correlation between PS and UCPCR was examined only in patients with CKD with a BMI > 25 or higher. PS did not correlate with insulin resistance in patients with high BMI, suggesting that renal insufficiency was still a contributing factor to insulin resistance (Fig. 5I).

Discussion

In our previous study, we found a negative correlation between the serum PS concentration and eGFR¹¹. PS, which accumulates due to renal dysfunction⁴⁵, exacerbates diabetic nephropathy by damaging podocytes. Accumulation of PS is both a consequence and a contributing factor to further renal impairment, underlining its significance in renal disease progression. In healthy mice, PS did not induce albuminuria, suggesting that the presence of DM is necessary for PS to trigger albuminuria. Furthermore, we discovered that PS exacerbated glycemic control by increasing insulin resistance in patients with CKD (eGFR < 60 mL/min/1.73 m²). It has been reported that higher insulin levels and insulin secretion in ESRD patients are mainly a response to impaired insulin sensitivity in order to maintain normal glucose regulation and decreased insulin clearance³. However, our results suggest that PS accumulation causes both elevated insulin levels and impaired insulin sensitivity is caused by itself¹¹. In terms of insulin secretion, experiments in healthy mice, KKAY-HF mice, cells, and cohorts of non-DM and DM patients have shown that PS acts on the pancreas to promote insulin secretion. Ddah2 and Prkag1, among others, may be involved in this pathway, and the results of RNA-seq pathway analysis suggest that PS acts on the pancreas to promote insulin secretion. Ddah2 is a promising target molecule for the treatment of diabetes as it regulates nitric oxide metabolism and the transcription of secretagogin through a Sirt1-dependent mechanism. The results from the GSIS assay conducted with Ddah2 KD revealed that PS acts as a Ddah2 activator, contributing to transient insulin secretion. This finding suggests that activating Ddah2 could potentially serve as a novel mechanism for developing insulin secretion-promoting drugs. Additionally, downregulation of Prkag1 and AMPK activates the mTOR pathway, leading to increased insulin secretion. Indeed, there are some reports suggesting a correlation between mitochondrial function and insulin secretion⁴⁶. Because, in our experimental system, PS did not alter the insulin content within β -cell (Fig. 3B), we propose that PS may serve an effector on enhancing secretory capacity of β -cell rather than insulin production.

Considering HbA1c as a reflection of chronic hyperglycemia and UCPCR as a reflection of chronic hyperinsulinemia, correlation analysis on these clinical cohorts suggests that PS is negatively associated with hyperglycemia independently of CKD, and PS is positively associated with hyperinsulinemia only in DKD patients. These findings highlight the potential of PS as a therapeutic agent against diabetes by targeting these genes. However, further studies are required to confirm the exact mechanisms by which PS affects insulin secretion, and to establish the safety and efficacy of PS as a treatment for diabetes.

Notably, PS is produced by the human gut microbiota, and we demonstrated that endogenous PS analogs can also enhance insulin secretion more efficiently than PS. These results suggest that PS could promote insulin secretion in patients with good renal function, and that PS analogs may have the potential to become new therapeutic agents for diabetes mellitus. RNA-seq results have revealed that PS impairs mitochondrial function, a finding consistent with our past research¹¹ and the known role of PS in oxidative stress⁴⁷. However, further investigation is needed to clarify the link between this mitochondrial impairment and insulin secretion. These findings highlight the need for deeper understanding of PS's impact on cellular metabolism and its implications in metabolic regulation.

In contrast, comparisons between healthy and KKAY-HF mice, as well as between cohorts of non-DM and DM patients, indicated that PS acts on insulin resistance in renal failure, especially in CKD. Previous studies have reported that renal insulin resistance is induced by renal failure and that PS may be the causative agent of this phenomenon. The phenomenon by which PS acts only on adipocytes in renal failure, suggesting insulin resistance, is thought to occur because PS remains in the body longer and acts on adipocytes more easily when renal function is reduced.

Our research also indicates that increased phosphorylation of Erk in adipocytes contributes to insulin resistance, a process typically linked to oxidative stress. We infer that oxidative stress, particularly induced by PS, plays a crucial role in this mechanism by promoting Erk phosphorylation^{48,49}. This suggests that PS-induced oxidative stress is a key factor in metabolic dysregulation, affecting insulin signaling in adipocytes. Our findings thus reveal a potential mechanistic pathway wherein PS not only exacerbates oxidative stress but also contributes to insulin resistance and metabolic disorders. Furthermore, the activation of Erk disrupts the regulation of adipocytokines¹³, including the malignant adipocytokine TNF- α , which also activates Erk⁵⁰. Therefore, PS may heighten the risk of insulin resistance and related diseases by initiating a cycle of Erk activation and abnormal adipocytokine release. Adipocytokines are considered one of the causes of many metabolic diseases, and their effects and impacts are being studied. It is well known that obesity confers an increased risk for serious metabolic diseases including type 2 diabetes, non-alcoholic fatty liver disease, and cardiovascular diseases. In addition, adipocytokines are thought to increase the risk of these diseases^{51,52}. Improvement of the gut microbiota by probiotics and other means may help ameliorate diabetes and reduce the risk of metabolic diseases by inhibiting PS and, consequently, Erk activation and adipocytokine release.

Our RNA-seq analysis revealed changes in the expression of several genes, including lncRNAs, in PS-treated 3T3-L1 derived adipocytes. Since lncRNAs have been implicated in adipogenesis and insulin resistance^{26–28}, these changes suggest that PS treatment may affect these cellular processes. Neat1 is involved in adipogenesis^{53,54} and may cause mitochondria impairment⁵⁵. Furthermore, changes in genes related to the cell cycle indicated the swelling of adipocytes, which was also observed in mouse tissues. We also reported that PS impairs mitochondrial function in podocyte¹¹ and that Neat1 may be a cause of this. Malat1 is also a lncRNA involved in adipogenesis⁵⁶. Further studies are required to understand the underlying mechanisms and the potential clinical implications of PS in metabolic disorders. We previously suggested that a tyrosine phenol-lyase (TPL) inhibitor, which blocks PS production by the gut microbiota, reduces the PS concentration in the serum and albuminuria in diabetic mice¹¹. PS induces insulin resistance in KKAY mice fed a high-fat diet and in human patients with CKD G3. Controlling PS production using TPL inhibitors may be a novel strategy for the treatment of insulin resistance and albuminuria in CKD.

One potential limitation of our study is the absence of fasting glucose and insulin level to estimate HOMA2-IR in the two DKD and CKD cohort examined. Here, to overcome this, we alternatively used urinary C-peptide/creatinine ratio (UCPCR)⁴³. Indeed, in this study, we found a significant correlation between blood PS concentration and insulin resistance using UCPCR. However, it is necessary to measure blood insulin levels to clarify more accurate relationships with hypertension and obesity. By examining the relationship in the future, it is thought that the relationship between PS, insulin secretion, and insulin resistance will be clarified.

In conclusion, our data highlighted that PS and endogenous sulfate metabolites that accumulated in CKD induced insulin secretion from β -cell, and PS also increased insulin resistance through lncRNAs expression and Erk phosphorylation in adipocytes, resulting in changes in glucose metabolism in CKD and DKD patients.

Methods and materials

Animal ethics and human ethics

ANIMAL ethics: All experiments involving animal use were approved with the Tohoku University Institutional Animal Care and Use Committee (2013-001-9). All methods were carried out in accordance with Tohoku University and national guidelines and regulations. Animal use was performed according to the ARRIVE guidelines (<https://arriveguidelines.org>).

HUMAN ethics: All procedures performed in studies involving human participants were in accordance with the ethical standards of the institutional and/or national research committee and with the Helsinki Declaration and its later amendments or comparable ethical standards. This study was approved by the Tohoku University Ethics Committee (2017-1-870) and Okayama University Ethics Committee (1702-026). Human samples were collected in accordance with the guidelines of Tohoku University (2017-1-870) and written informed consent was obtained from Okayama University (UMIN 00011525 and 1702-026).

Material details

PS was synthesized by Sundia MediTech (Shanghai, China) and ISOTEC (Sigma-Aldrich, Burlington, MA). Phenol analogs were chemically synthesized.

Animal experiments

All male C57BL/6N and KKAY mice were obtained from CLEA (Tokyo, Japan) at 4 weeks old and acclimated for 2 weeks in a controlled environment. The mice were housed in cages under standard laboratory conditions, maintained at a temperature of $22 \pm 2^\circ\text{C}$, with a relative humidity of $50 \pm 10\%$, and on a 12-hour light/dark cycle. Mice had free access to tap water and standard chow unless otherwise specified. KKAY mice were fed a high-fat diet (15.3% fat, 424.5 cal/100 g; Quick fat, CLEA, Tokyo, Japan) and had free access to tap water. PS intake was estimated (50 mg/kg/day) by measuring the amount of water intake. PS was administered with 0.1% PS included water for 5 weeks. Urinary albumin levels were determined by ELISA (Exocell Inc., Philadelphia, PA). To ensure the robustness of the results, randomization was applied when assigning mice to experimental groups. Investigators were blinded to the group allocation during the data collection and analysis phases to reduce potential bias. At the end of the experiments, mice were euthanized using isoflurane inhalation anesthesia (3–5% for induction and 1.5–2% for maintenance), followed by cervical dislocation to ensure humane endpoints. Isoflurane was administered using an anesthetic vaporizer to control the concentration precisely and minimize stress to the animals. This method was chosen due to its rapid induction, reversibility, and suitability for small animals, ensuring minimal pain and distress.

Glucose tolerance test (GTT) and insulin tolerance test (ITT)

GTT and ITT were performed as previously described¹⁶ with $n = 3$ –5. Briefly, an oral glucose tolerance test (GTT) was performed after overnight fasting, with ad libitum access to water. Glucose (2 g/kg) was administered intraperitoneally. For insulin tolerance testing (ITT), 8-hour fasted mice were intraperitoneally injected with regular human insulin (2 U/kg body weight). Blood samples were collected from the retro-orbital sinus at 15, 30, 60, and 120 min. Each blood sample was centrifuged, and the plasma was removed and stored at -20°C until analysis of glucose and insulin concentrations. The glucose and insulin concentrations were measured according to the manufacturer's instructions (Wako Pure Chemical, Osaka, Japan).

Histological examination

The pancreas and white adipose tissue (WAT) were fixed in 10% neutral buffered formalin and embedded in paraffin. Pancreatic sections were stained with anti-insulin antibody (1:1000, #I2018, Sigma, Burlington, MA). WAT sections were stained with hematoxylin and eosin (HE). The images were captured and processed using a BZ-X810 fluorescence microscope (KEYENCE, Osaka, Japan), using a Plan Apochromat 10x objective (NA0.45, BZ-PA10, KEYENCE, Osaka, Japan). The BZ-X810 Analyzer software was used for the extraction and quantification of insulin-positive areas and quantification of WAT as the number of cells per unit area. The area of mesangial region was measured in HE staining with ImageJ software (Version 1.54, National Institutes of Health).

Cell culture

INS-1e cells¹⁶ were grown in RPMI-1640 medium with no glucose in Primaria flask (#353810, Corning, Corning, NY). 3T3-L1 cells were grown in DMEM (high glucose) with 10% fetal bovine serum (FBS). Adipocyte differentiation was performed as follows: AdipoInducer Reagent (#MK429, Takara, Shiga, Japan) were used to differentiate and maintain as an adipocyte. In detail, insulin (10 $\mu\text{g/mL}$), dexamethasone (2.5 μM) and 3-isobutyl-1-methylxanthine solution (0.5 μM) were used for differentiation, and insulin (10 $\mu\text{g/mL}$) was further used for maintenance.

Ddah2 knock down with siRNA and quantitative real-time PCR

To knock down the Ddah2, siRNA (Cat #4351372; Thermo Fisher Scientific, Waltham, MA) were transfected into INS-1e cells with RNAiMAX-lipodectamine (Invitrogen, Waltham, MA) and Opti-MEM-I (Gibco, Waltham, MA) by reverse transfection method. After checked the down expression level of Ddah2 with qPCR and western blotting, GSIS was performed. qPCR was performed with the Taqman primer (Ddah2: Rn03993445_g1, Cat# 4351372, Gapdh: Rn01775763_g1, Cat# 4308313, Thermo Fisher Scientific, Waltham, MA). Total RNA was extracted by RNeasy plus mini kit (Qiagen, Hilden, Germany). cDNA ($n=4$) was synthesized using a ReverTra Ace qPCR RT Kit (TOYOBO, Osaka, Japan). Quantitative real-time PCR was performed according to the manufacturer's instructions on a StepOnePlus™ Real Time PCR System (Thermo Fisher Scientific, Waltham, MA). The cycle threshold (Ct) was calculated using the Ct method. The relative mRNA expression levels were normalized to that of Gapdh.

Effects of phenol analogs on glucose-stimulated insulin secretion (GSIS)

GSIS was measured as previously reported¹⁶. Briefly, approximately 80% confluent INS-1e cells in 96 well plates were incubated in the presence or absence of PS or a phenyl analog for 24 h. Cells were then maintained for 1 h, washed twice, and preincubated at 37 °C for 1 h in a buffer containing (in mM): 135 NaCl, 3.6 KCl, 5 NaHCO₃, 0.5 NaH₂PO₄, 0.5 MgCl₂, 1.5 CaCl₂, 10 HEPES, and 0.1% BSA 0.1%, pH 7.4. The cells were then incubated in buffer containing glucose for 1 h. The insulin concentration was measured using a rat insulin ELISA kit (Mercodia, Uppsala, Sweden).

Measurement of insulin secretion from isolated islets, and their protein content

The isolation of islets and the measurement of insulin secretion from islets were performed as described¹⁹. Briefly, groups of 10 islets were initially incubated in Krebs Ringer bicarbonate solution (KRB) with 2.8 mM glucose for one hour at 37 °C in an atmosphere of 95% O₂ and 5% CO₂. Following this, they were incubated for another hour in 0.1 mL of fresh KRB, but this time with varying glucose concentrations. Separately, cells (100,000 cells per well in a 48 well plate) were seeded and grown in DMEM for two days, then treated with or without 100 μM PS. On the experiment day, these cells were immersed in a 2-(4-[2-hydroxyethyl]ff-1-piperazine) ethanesulfonic acid (HEPES)-balanced KRB solution (KRH), which included 119 mM NaCl, 4.7 mM KCl, 2.5 mM CaCl₂, 1.2 mM MgCl₂, 1.2 mM KH₂PO₄, 25 mM NaHCO₃, and 20 mM HEPES, pH 7.4. This solution was also supplemented with 5 mg/mL BSA and 2.8 mM glucose and maintained at 37 °C for two hours. Afterwards, they were incubated in fresh KRH with different glucose or KCl concentrations for two hours. Post incubation, the medium was removed from the islets or cells, and the insulin levels in the medium were measured using an insulin ELISA kit (Morinaga Institute of Biological Science, Yokohama, Japan). Additionally, the total protein content of the islets or cells was quantified using the Micro-BCA Protein Assay Reagent (PIERCE Biotechnology Inc., Rockford, IL).

RNA sequencing

Total RNA was extracted by RNeasy plus mini kit (Qiagen, Hilden, Germany). RNA sequence library preparation was performed using a QIAseq Stranded RNA Library Kit (Qiagen, Hilden, Germany), according to the manufacturer's instructions. Sequencing was performed by DNAFORM (Yokohama, Kanagawa, Japan). Sequence reads in Fastq format were assessed for quality using FastQC. Raw reads were filtered to remove low-quality reads using Trimmomatic-0.39. The obtained reads were mapped to mouse GRCm39 and mRatBN7.2/rn7 genomes using STAR (version 2.7.10a). Reads on annotated genes were counted using StringTie software (v2.2.0). Gene expression levels were measured using the Bioconductor package, edgeR (version 3.15).

Phosphorylation assay

3T3-L1 derived adipocytes were plated in 96 well plates and grown until they reached 90% confluence with adipocyte maintenance medium (DMEM, high glucose, 10% FBS and 2.5 μM insulin). After 6 h of FBS and insulin starvation, cells were treated with PS (10 μM) for 1 hour. Cells were then stimulated with insulin (100 nM) for 30 min. The cell monolayers were treated as described in the text and processed using the ERK1/2 (pT202/Y204 + Total) ELISA Kit (Cat #ab176660, Abcam, Cambridge, UK), following the manufacturer's guidelines, and adding the HALT protease and phosphatase inhibitor cocktail (Thermo Fisher Scientific, Waltham, MA) was added to the lysis buffer provided in the kit. The results were read on a Spectramax 190 (Molecular Devices, San Jose, CA) and analyzed as the pErk/total Erk signal ratio⁵⁷.

Western blotting

3T3-L1 derived adipocytes expressing myc-GLUT4-EGFP were serum-starved for 3 h, washed thrice with KRPH buffer, and stimulated with insulin (0–200 nM) for 30 min in the presence or absence of PS (10 μM) for 60 min. Phosphorylation of protein kinase B (Akt; Ser473) and Erk was analyzed by western blotting as described previously⁵⁸. Antibodies used were obtained from Ddah2 (1:1000, #14966-1-AP, PGI), Myc (1:1000, Cat #16-263, Sigma Aldrich, St.Louis, MO), P-Akt (S473) (1:1000, Cat #9271, Cell Signaling Technology, Danvers, MA), Sortilin (1:2000, Cat #12369-1-AP, Proteintech, Rosemont, IL), β actin (1:1000, Cat #5125, Cell Signaling Technology, Danvers, MA), and Gapdh (1:1000, Cat #ab9485, Abcam, Cambridge, United Kingdom).

Recruitment and measurement of the U-CARE cohort study10

The Urinary Biomarker for Continuous and Rapid Progression of Diabetic Nephropathy (U-CARE) study is a multicenter, observational clinical study that aimed to investigate urinary biomarkers in diabetic nephropathy (UMIN 00011525). The U-CARE assay was performed as previously described¹¹. We recruited 362 patients (U-CARE, registered at UMIN 00011525). The protocol was following: The estimated GFR (eGFR) was calculated according to sex, age, and serum Cre concentration using the Japanese Chronic Kidney Disease Epidemiology

Collaboration (CKD-EPI). U-CARE urine C-peptide levels were measured by ELISA using a C-peptide ELISA kit (Mercodia, Uppsala, Sweden), according to the manufacturer's instructions.

Recruitment and measurement of the non-DM cohort

We recruited 100 patients treated at the outpatient clinic of the Tohoku University Hospital. The study protocol was approved by the Ethics Committee of Tohoku University (2022-1-823, 2012-3-19) and complied with the guidelines of the Declaration of Helsinki. Written informed consent was obtained from all the patients. Urinary C-peptide levels were measured by ELISA using a C-peptide ELISA kit (Mercodia, Uppsala, Sweden), according to the manufacturer's instructions.

Quantification of PS by LC/MS/MS

PS levels in animal plasma were measured as we recently reported⁵⁹. Deuterated internal standards were used for all analytes, and a TSQ Quantum Ultra triple quadrupole mass spectrometer (Thermo Fisher Scientific, Waltham, MA) equipped with a heated ESI source system was used. The mass spectrometer was operated in both the positive and negative ionization modes. The samples were analyzed in single reaction monitoring mode by monitoring the ion transitions at m/z 173.0 \rightarrow 93.3 PS. Data were acquired and analyzed using the Xcalibur™ software (version 2.1, Thermo Scientific, Waltham, MA). For human samples, the PS level in fresh-frozen plasma was measured by LSI Medience Co. (Tokyo, Japan) using another method to help clinicians measure the PS. Briefly, LC-MS/MS datasets were acquired using a liquid chromatograph Nexera X2 LC0AD equipped with an ESI and triple quadrupole mass spectrometer 8050 (Shimadzu, Kyoto, Japan). The mass spectrometer was operated in the negative mode. Data acquisition and analysis were performed using Shimadzu Lab Solutions version 5.89. The correlation between each measurement was confirmed to be greater than 0.99269.

Statistical analysis

To normalize the data distribution in clinical data analysis, $\log(\text{PS} + 1)$ transformation was applied. Data are presented as mean \pm standard error. Statistical significance was determined using the Student's *t*-test. A *p*-value significance was set at <0.05 . Prior to applying the Student's *t*-test, the data distribution was assessed using the Shapiro-Wilk test to confirm normality. For RNA-seq data analysis, false discovery rate (FDR) correction was applied to control for multiple comparisons, and adjusted *p*-values <0.05 were considered significant. GraphPad Prism 9 (Version 9.5.1) (GraphPad Software, Boston, MA) was used for statistical analyses.

Data availability

The datasets generated during the current study are deposited to the NCBI Read Archive (SRA) and available under the accession number PRJNA1026807.

Received: 17 February 2024; Accepted: 20 January 2025

Published online: 17 February 2025

References

- Pina, A. F. et al. Insulin: trigger and target of renal functions. *Front. Cell. Dev. Biol.* **8**, 519. <https://doi.org/10.3389/fcell.2020.00519> (2020).
- de Boer, I. H. et al. Impaired glucose and insulin homeostasis in moderate-severe CKD. *J. Am. Soc. Nephrol.* **27**, 2861–2871. <https://doi.org/10.1681/ASN.2015070756> (2016).
- Guthoff, M. et al. Impact of end-stage renal disease on glucose metabolism—a matched cohort analysis. *Nephrol. Dial. Transpl.* **32**, 670–676. <https://doi.org/10.1093/ndt/gfx018> (2017).
- Grube, D. et al. Insulin use in chronic kidney disease and the risk of hypoglycemic events. *BMC Nephrol.* **23**, 73. <https://doi.org/10.1186/s12882-022-02687-w> (2022).
- Keigo Yasuda, M. D. et al. Relationship Between Insulin Response to Oral Glucose Load and Creatinine Clearance. *Diabetes* **24**(12), 1066–1071. <https://doi.org/10.2337/diab.24.12.1066> (1975).
- Ahmad, I. et al. Hypoglycemia in people with type 2 diabetes and CKD. *Clin. J. Am. Soc. Nephrol.* **14**, 844–853. <https://doi.org/10.2215/CJN.11650918> (2019).
- Hassan, N. K. et al. A clinical review on Nutritional requirements and Assessment for type 2 diabetes Mellitus with Chronic Renal Disease. *Curr. Diabetes Rev.* **16**, 922–930. <https://doi.org/10.2174/157339981666620021120402> (2020).
- Becker, B. et al. Renal insulin resistance syndrome, adiponectin and cardiovascular events in patients with kidney disease: the mild and moderate kidney disease study. *J. Am. Soc. Nephrol.* **16**, 1091–1098. <https://doi.org/10.1681/ASN.2004090742> (2005).
- Tuttle, K. R. et al. Diabetic kidney disease: a report from an ADA Consensus Conference. *Am J Kidney Dis* **64**, 510–533, (2014). <https://doi.org/10.1053/j.ajkd.2014.08.001>
- Mohandes, S. et al. Molecular pathways that drive diabetic kidney disease. *J. Clin. Invest.* **133** <https://doi.org/10.1172/JCI165654> (2023).
- Kikuchi, K. et al. Gut microbiome-derived phenyl sulfate contributes to albuminuria in diabetic kidney disease. *Nat. Commun.* **10**, 1835. <https://doi.org/10.1038/s41467-019-09735-4> (2019).
- Meier, J. J. et al. Functional assessment of pancreatic beta-cell area in humans. *Diabetes* **58**, 1595–1603. <https://doi.org/10.2337/db08-1611> (2009).
- Ozaki, K. I. et al. Targeting the ERK signaling pathway as a potential treatment for insulin resistance and type 2 diabetes. *Am. J. Physiol. Endocrinol. Metab.* **310**, E643–E651. <https://doi.org/10.1152/ajpendo.00445.2015> (2016).
- Guillermier, C. et al. Imaging mass spectrometry demonstrates age-related decline in human adipose plasticity. *JCI Insight.* **2**, e90349. <https://doi.org/10.1172/jci.insight.90349> (2017).
- Kim, S. M. et al. Loss of white adipose hyperplastic potential is associated with enhanced susceptibility to insulin resistance. *Cell. Metab.* **20**, 1049–1058. <https://doi.org/10.1016/j.cmet.2014.10.010> (2014).
- Abe, M. et al. The HMG-CoA reductase inhibitor pravastatin stimulates insulin secretion through organic anion transporter polypeptides. *Drug Metab. Pharmacokinet.* **25**, 274–282. <https://doi.org/10.2133/dmpk.25.274> (2010).
- Santini, E. et al. Effect of PPAR- γ activation and inhibition on glucose-stimulated insulin release in INS-1E cells. *Diabetes* **53** (Suppl 3), 79–83. https://doi.org/10.2337/diabetes.53.suppl_3.s79 (2004).

18. Yamamoto, S. et al. Continuous reduction of protein-bound uremic toxins with improved oxidative stress by using the oral Charcoal Adsorbent AST-120 in Haemodialysis patients. *Sci. Rep.* **5**, 14381. <https://doi.org/10.1038/srep14381> (2015).
19. Takahashi, I., Ohashi, K. & Nata, K. Involvement of heparan sulfate 3-O-sulfotransferase isoform-1 in the insulin secretion pathway. *J. Diabetes Investig.* **3**, 362–370. <https://doi.org/10.1111/j.2040-1124.2012.00205.x> (2012).
20. Toyohara, T. et al. Metabolomic profiling of uremic solutes in CKD patients. *Hypertens. Res.* **33**, 944–952. <https://doi.org/10.1038/hr.2010.113> (2010).
21. Tabrett, C. A. & Coughtrie, M. W. Phenol sulfotransferase 1A1 activity in human liver: kinetic properties, interindividual variation and re-evaluation of the suitability of 4-nitrophenol as a probe substrate. *Biochem. Pharmacol.* **66**, 2089–2097. [https://doi.org/10.1016/S0006-2952\(03\)00582-3](https://doi.org/10.1016/S0006-2952(03)00582-3) (2003).
22. Tanaka, H., Sirich, T. L., Plummer, N. S., Weaver, D. S. & Meyer, T. W. An Enlarged Profile of Uremic Solutes. *PLoS One*. **10**, e0135657. <https://doi.org/10.1371/journal.pone.0135657> (2015).
23. Hasegawa, K. et al. The hydrolase DDAH2 enhances pancreatic insulin secretion by transcriptional regulation of secretagogin through a Sirt1-dependent mechanism in mice. *FASEB J.* **27**, 2301–2315. <https://doi.org/10.1096/fj.12-226092> (2013).
24. Inoki, K., Kim, J. & Guan, K. L. AMPK and mTOR in cellular energy homeostasis and drug targets. *Annu. Rev. Pharmacol. Toxicol.* **52**, 381–400. <https://doi.org/10.1146/annurev-pharmtox-010611-134537> (2012).
25. Kubi, J. A. et al. Effects of 2,3,7,8-tetrachlorodibenzo-p-dioxin (TCDD) on the differentiation of embryonic stem cells towards pancreatic lineage and pancreatic beta cell function. *Environ Int* **130**, 104885. (2019). <https://doi.org/10.1016/j.envint.2019.05.079>
26. Han, M. et al. RNA-sequencing analysis reveals the potential contribution of lncRNAs in palmitic acid-induced insulin resistance of skeletal muscle cells. *Biosci. Rep.* **40** <https://doi.org/10.1042/BSR20192523> (2020).
27. Chen, C. et al. Long non-coding RNAs regulation in adipogenesis and lipid metabolism: emerging insights in obesity. *Cell. Signal.* **51**, 47–58. <https://doi.org/10.1016/j.cellsig.2018.07.012> (2018).
28. Squillaro, T., Peluso, G., Galderisi, U. & Di Bernardo, G. Long non-coding RNAs in regulation of adipogenesis and adipose tissue function. *Elife* **9** <https://doi.org/10.7554/eLife.59053> (2020).
29. Nakatsuka, A., Wada, J. & Makino, H. Cell cycle abnormality in metabolic syndrome and nuclear receptors as an emerging therapeutic target. *Acta Med. Okayama.* **67**, 129–134. <https://doi.org/10.18926/AMO/50405> (2013).
30. James, D. E., Brown, R., Navarro, J. & Pilch, P. F. Insulin-regulatable tissues express a unique insulin-sensitive glucose transport protein. *Nature* **333**, 183–185. <https://doi.org/10.1038/333183a0> (1988).
31. Shepherd, P. R. & Kahn, B. B. Glucose transporters and insulin action—implications for insulin resistance and diabetes mellitus. *N Engl. J. Med.* **341**, 248–257. <https://doi.org/10.1056/NEJM199907223410406> (1999).
32. Nedachi, T. & Kanzaki, M. Regulation of glucose transporters by insulin and extracellular glucose in C2C12 myotubes. *Am. J. Physiol. Endocrinol. Metab.* **291**, E817–E828. <https://doi.org/10.1152/ajpendo.00194.2006> (2006).
33. Fujita, H. et al. Identification of three distinct functional sites of insulin-mediated GLUT4 trafficking in adipocytes using quantitative single molecule imaging. *Mol. Biol. Cell.* **21**, 2721–2731. <https://doi.org/10.1091/mbc.E10-01-0029> (2010).
34. Cong, L. N. et al. Physiological role of Akt in insulin-stimulated translocation of GLUT4 in transfected rat adipose cells. *Mol. Endocrinol.* **11**, 1881–1890. <https://doi.org/10.1210/mend.11.13.0027> (1997).
35. Kaddai, V. et al. Involvement of TNF-alpha in abnormal adipocyte and muscle sortilin expression in obese mice and humans. *Diabetologia* **52**, 932–940. <https://doi.org/10.1007/s00125-009-1273-3> (2009).
36. Blondeau, N., Beraud-Dufour, S., Lebrun, P., Hivelin, C. & Coppola, T. Sortilin in glucose homeostasis: from accessory protein to Key Player? *Front. Pharmacol.* **9**, 1561. <https://doi.org/10.3389/fphar.2018.01561> (2018).
37. Li, J. et al. Inhibition of insulin/PI3K/AKT signaling decreases adipose Sortilin 1 in mice and 3T3-L1 adipocytes. *Biochim. Biophys. Acta Mol. Basis Dis.* **1863**, 2924–2933. <https://doi.org/10.1016/j.bbdis.2017.08.012> (2017).
38. Koppe, L. et al. p-Cresyl sulfate promotes insulin resistance associated with CKD. *J. Am. Soc. Nephrol.* **24**, 88–99. <https://doi.org/10.1681/ASN.2012050503> (2013).
39. Mise, K. et al. Identification of novel urinary biomarkers for Predicting Renal prognosis in patients with type 2 diabetes by glycan profiling in a Multicenter prospective cohort Study: U-CARE Study 1. *Diabetes Care.* **41**, 1765–1775. <https://doi.org/10.2337/dc18-0030> (2018).
40. Mise, K. et al. Novel urinary glycan biomarkers Predict Cardiovascular events in patients with type 2 diabetes: a Multicenter prospective study with 5-Year follow up (U-CARE study 2). *Front. Cardiovasc. Med.* **8**, 668059. <https://doi.org/10.3389/fcvm.2021.668059> (2021).
41. Koenig, R. J. et al. Correlation of glucose regulation and hemoglobin A1c in diabetes mellitus. *N Engl. J. Med.* **295**, 417–420. <https://doi.org/10.1056/NEJM197608192950804> (1976).
42. Matthews, D. R. et al. Homeostasis model assessment: insulin resistance and beta-cell function from fasting plasma glucose and insulin concentrations in man. *Diabetologia* **28**, 412–419. <https://doi.org/10.1007/BF00280883> (1985).
43. Wang, Y. et al. Urinary C-peptide/creatinine ratio: a useful biomarker of insulin resistance and refined classification of type 2 diabetes mellitus. *J. Diabetes.* **13**, 893–904. <https://doi.org/10.1111/1753-0407.13203> (2021).
44. Kikuchi, K. et al. Metabolomic analysis of uremic toxins by liquid chromatography/electrospray ionization-tandem mass spectrometry. *J. Chromatogr. B Analyt. Technol. Biomed. Life Sci.* **878**, 1662–1668. <https://doi.org/10.1016/j.jchromb.2009.11.040> (2010).
45. Velenosi, T. J. et al. Untargeted plasma and tissue metabolomics in rats with chronic kidney disease given AST-120. *Sci. Rep.* **6**, 22526. <https://doi.org/10.1038/srep22526> (2016).
46. Maechler, P. Mitochondrial function and insulin secretion. *Mol. Cell. Endocrinol.* **379**, 12–18. <https://doi.org/10.1016/j.mce.2013.06.019> (2013).
47. Edamatsu, T., Fujieda, A. & Itoh, Y. Phenyl sulfate, indoxyl sulfate and p-cresyl sulfate decrease glutathione level to render cells vulnerable to oxidative stress in renal tubular cells. *PLoS One*. **13**, e0193342. <https://doi.org/10.1371/journal.pone.0193342> (2018).
48. Nowak, G., Clifton, G. L., Godwin, M. L. & Bakajsova, D. Activation of ERK1/2 pathway mediates oxidant-induced decreases in mitochondrial function in renal cells. *Am. J. Physiol. Ren. Physiol.* **291**, F840–F855. <https://doi.org/10.1152/ajprenal.00219.2005> (2006).
49. Khan, A. U. H. et al. Mitochondrial complex I activity signals antioxidant response through ERK5. *Sci. Rep.* **8**, 7420. <https://doi.org/10.1038/s41598-018-23884-4> (2018).
50. Chang, E. et al. Restoration of adiponectin expression via the ERK pathway in TNFalpha-treated 3T3-L1 adipocytes. *Mol. Med.* **10**, 905–910. <https://doi.org/10.3892/mmr.2014.2278> (2014).
51. Cao, H. Adipocytokines in obesity and metabolic disease. *J. Endocrinol.* **220**, T47–59. <https://doi.org/10.1530/JOE-13-0339> (2014).
52. Landecho, M. F. et al. Relevance of Leptin and Other Adipokines in Obesity-Associated Cardiovascular Risk. *Nutrients* **11**, (2019). <https://doi.org/10.3390/nu11112664>
53. Wei, S. et al. Long noncoding RNAs in regulating adipogenesis: new RNAs shed lights on obesity. *Cell. Mol. Life Sci.* **73**, 2079–2087. <https://doi.org/10.1007/s00018-016-2169-2> (2016).
54. Gernapudi, R. et al. MicroRNA 140 promotes expression of long noncoding RNA NEAT1 in Adipogenesis. *Mol. Cell. Biol.* **36**, 30–38. <https://doi.org/10.1128/MCB.00702-15> (2016).
55. Zhang, H. et al. LncRNA NEAT1 controls the lineage fates of BMSCs during skeletal aging by impairing mitochondrial function and pluripotency maintenance. *Cell. Death Differ.* **29**, 351–365. <https://doi.org/10.1038/s41418-021-00858-0> (2022).
56. Han, J. et al. The long noncoding RNA MALAT1 modulates adipose loss in cancer-associated cachexia by suppressing adipogenesis through PPAR-gamma. *Nutr. Metab. (Lond)*. **18**, 27. <https://doi.org/10.1186/s12986-021-00557-0> (2021).

57. Patrone, M. et al. Combinatorial allosteric modulation of agonist response in a self-interacting G-protein coupled receptor. *Commun. Biol.* **3**, 27. <https://doi.org/10.1038/s42003-020-0752-4> (2020).
58. Shima, H. et al. A novel indole compound MA-35 attenuates renal fibrosis by inhibiting both TNF- α and TGF- β 1 pathways. *Sci. Rep.* **7**, 1884. <https://doi.org/10.1038/s41598-017-01702-7> (2017).
59. Kanemitsu, Y. et al. Simultaneous quantitative analysis of uremic toxins by LC-MS/MS with a reversed-phase/cation-exchange/anion-exchange tri-modal mixed-mode column. *J. Chromatogr. B Analyt Technol. Biomed. Life Sci.* **1068–1069**, 1–8. <https://doi.org/10.1016/j.jchromb.2017.10.009> (2017).

Acknowledgements

We thank Fumiko Date, Miki Yoshizawa, Naoko Shibata, and Chika Tazawa (Histological platform, Tohoku University School of Medicine) for their histological assistance and Biomedical Research Core of Tohoku University Graduate School of Medicine. This work was supported in part by the National Grant-in-Aid for Scientific Research from the Ministry of Education, Culture, Sports, Science, and Technology of Japan (18H02822), the Japan Agency for Medical Research and Development (AMED) 20ek0210133h0001, 20ak0101127h0001, and JP22zf0127001, 24zf0127001h0004, Okinaka memorial institute for medical research and Anzai memorial diabetes research grant by Gonryo for the promotion of medical science.

Author contributions

Y.T. and T.A. participated in the conception and design of the study, Y.T., T.K., T.S., C.K., Y.M., and K.S. performed in vitro experiments, Y.T. analyzed in vitro, in vivo data, and clinical data. Y.T. and T.A. wrote the manuscript. Funding were acquired by T.A., Y.T., and T.K. T.K. performed RNA-seq and analyzed the data. Y.A., H.J.H. and K.K. performed in vivo experiments. Y.M., R.K., and Y.T. measured uremic toxins. T.A., T.T., and J.W. collected the clinical information. T.A. oversaw data collection and interpretation. M.K., K.N., T.K., S.W., K.K., T.T., T.S., and T.A. contributed to writing the discussion. All authors read and approved the final manuscript.

Declarations

Competing interests

The authors declare no competing interests.

Additional information

Supplementary Information The online version contains supplementary material available at <https://doi.org/10.1038/s41598-025-87501-x>.

Correspondence and requests for materials should be addressed to T.A.

Reprints and permissions information is available at www.nature.com/reprints.

Publisher's note Springer Nature remains neutral with regard to jurisdictional claims in published maps and institutional affiliations.

Open Access This article is licensed under a Creative Commons Attribution-NonCommercial-NoDerivatives 4.0 International License, which permits any non-commercial use, sharing, distribution and reproduction in any medium or format, as long as you give appropriate credit to the original author(s) and the source, provide a link to the Creative Commons licence, and indicate if you modified the licensed material. You do not have permission under this licence to share adapted material derived from this article or parts of it. The images or other third party material in this article are included in the article's Creative Commons licence, unless indicated otherwise in a credit line to the material. If material is not included in the article's Creative Commons licence and your intended use is not permitted by statutory regulation or exceeds the permitted use, you will need to obtain permission directly from the copyright holder. To view a copy of this licence, visit <http://creativecommons.org/licenses/by-nc-nd/4.0/>.

© The Author(s) 2025